Reducing Uncertainty With Seismic Measurements While Drilling

Hugues Djikpesse, *Member, IEEE*, Phil Armstrong, Rogelio Rufino, and Andy Hawthorn

***Abstract*—This paper discusses both seismic checkshot data inversion and seismic waveform look-ahead imaging while drilling. We investigate the estimation under real-time data uncertainties of interval velocity profiles calculated from checkshot measurements acquired while drilling. It is found that real-time checkshots may suffer from downhole time-picking errors in addition to an unpredictable clock drift uncertainty. We developed a method to account for these uncertainties and to provide drillers with reliable formation interval velocity models in real time, regardless of whether the direct arrival times are detected by an automated downhole process or picked by an interpreter uphole once the seismograms have been transmitted to the surface through mud-pulse telemetry. By quantifying the posterior uncertainties in the interpreted velocity measurements, we then demonstrate: 1) the value of making the seismic waveforms recorded in downhole memory available in real time at the surface and 2) the benefit of quantifying and accounting for the standard deviations, which describe the downhole time-picking errors, in the case when the real-time seismograms are not available. This is exemplified with the application of the proposed methodology to measurements collected in deep water in the Gulf of Mexico, with inverted real-time velocity models that are consistent and comparable to the ones obtained from travel times picked after the drilling is complete. Finally, a case study is shown combining real-time checkshot inversion and downhole-to-surface transmitted seismic waveforms to look ahead while drilling for an optimal well steering in high-probability hydrocarbon sands.**

***Index Terms*—Checkshot data acquisition, clock drift, downhole processing, geosteering, real-time applications, seismic while drilling (SWD), time-picking errors, uncertainty estimation.**

I. Introduction

MEASUREMENT while drilling (MWD) is a fast-growing service in the oil industry, aiming at collecting and analyzing in real time relevant information that might impact drilling operational decisions. Of particular interest are seismic-while-drilling (SWD) measurements: real-time checkshot and downhole-to-surface transmitted waveforms. Provided that accurate velocity profiles are available, real-time seismic waveforms are desirable to image ahead of the drill bit (look-ahead depth imaging) for efficient well steering; this includes avoiding hazardous situations such as unpredicted pressure anomalies that might cause catastrophic well collapses. This paper is an extension of a previous work [1] that only focused on checkshot inversion under real-time drilling uncertainties. In addition to checkshot inversion examples, this paper presents field cases highlighting the use of SWD real-time waveforms for optimal and cost-effective well steering.

Real-time checkshot data acquired while drilling consist of pairs of time-versus-depth values measuring the one-way time (OWT) that acoustic seismic waves travel, assuming vertical incidence from a surface source, to reach receivers located downhole in the drill collar close to the bottom hole assembly. They provide drillers with real-time information on the interval velocity of the formation surrounding the wellbore and on the position of the bit on the surface seismic time section. This helps in placing the drill bit with respect to the geology, calibrating logging-while-drilling (LWD) sonic data, monitoring changes in interval velocity profiles, and making cost-effective decisions such as optimizing casing points. Indeed, the number of casing points directly controls the size of the hole and, therefore, the future hydrocarbon production (or water injection) flow rates of the targeted wells. In addition, the interval velocity may be used to calibrate predrill pore pressure predictions and, in the case of pressure ramps that cover an extended depth interval, may even directly serve for "relevant-time" control of mud weight.

The estimation of formation interval velocities from wireline vertical-seismic-profile (VSP) travel times has extensively been studied, particularly assuming randomly distributed and uncorrelated measurement errors (e.g., [2]–[7]). These are acquired after drilling and thus do not require real-time processing. However, little is available in the literature about travel-time inversion while drilling. However, successful drilling operations are largely determined by how risks have been assessed and mitigated in real time. It is therefore desirable to accurately predict, with meaningful uncertainties, formation interval velocity profiles while drilling.

Fig. 1 shows a typical real-time checkshot acquisition system. A synchronized dual-clock system is used for acquisition timing, while measurements acquired while drilling are processed downhole before being sent to the surface through mud-pulse telemetry (e.g., [8]). The surface equipment includes an airgun system (with sources of high-pressure air), a GPS-based navigation system (allowing to dynamically position the source vessel when sources are fired away from the rig), and a well-site processing equipment (typically set up in the wireline

Manuscript received September 30, 2008; revised February 5, 2009. First published September 22, 2009; current version published December 9, 2009. The Associate Editor coordinating the review process for this paper was Dr. Dario Petri.

H. Djikpesse is with the Department of Mathematics and Modeling, Schlumberger-Doll Research Center, Cambridge, MA 02139 USA (e-mail: HDjikpesse@slb.com).

P. Armstrong is with the Department of Acoustics Instrumentation, Schlumberger, Tokyo 104-0028, Japan.

R. Rufino is with Schlumberger Data and Consulting Services, Houston, TX 77077 USA.

A. Hawthorn is with Schlumberger Drilling and Measurements, Sugar Land, TX 77478 USA.

Color versions of one or more of the figures in this paper are available online at http://ieeexplore.ieee.org.

Digital Object Identifier 10.1109/TIM.2009.2025684

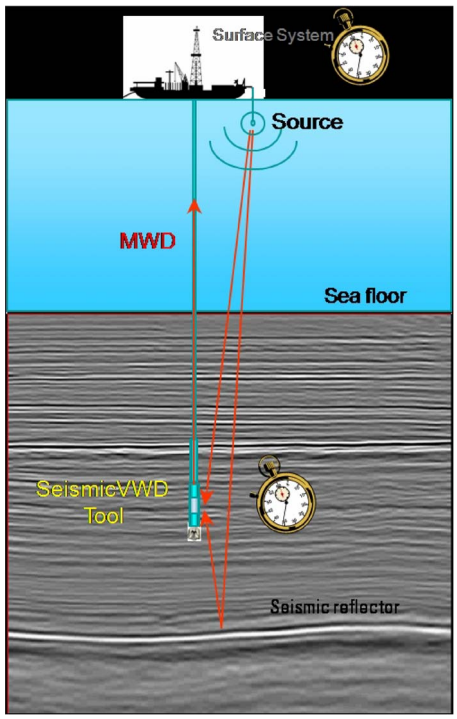

Fig. 1. Typical checkshot acquisition geometry with a surface source firing near the well head, while receivers located downhole record the acoustic first arrival travel times.

unit for a good view of the rig floor). Prior to running in hole, the entire system operation (including the synchronization of the dual-clock system) is systematically tested during a shallow-hole test.

For many years, real-time checkshot measurements have suffered from two major errors: 1) time-picking errors due to the automated downhole processing and 2) an unpredictable drift of the downhole clock submitted to high temperatures and pressures as compared to the clock that remained at the surface. Unfortunately, clock drift uncertainty was ignored, and the downhole picking standard deviation errors were defaulted to the nominal time resolution of the recorded waveforms, which is typically 2 ms. Only recently, [9] has provided a major breakthrough by managing to send the raw seismic waveforms uphole, despite the limited mud-pulse telemetry rates, for an accurate human-guided time picking.

This paper aims at valuing, in a quantitative way, recent technology breakthroughs associated with seismic data interpretation while drilling. We wish to estimate, based on data sets collected several years ago in the Gulf of Mexico, how much uncertainty reduction is gained between the original interpretations and those made today. To that end, we start in the next section by extending the work presented in [1] with a review of the mathematical background underlying seismic time-versus-depth mapping (generally known as seismic tomography). Using a forward modeling approach, we further exemplify the depth errors that might be introduced by considering various relative errors in the velocity profile. Section III is devoted to analyzing SWD data collected a few years ago to illustrate the different sources of uncertainty that might prevent accurate and meaningful interval velocity estimation. An inversion method is then developed, in Section IV, to estimate velocity models from real-time checkshot data collected in the presence of both picking errors and clock drift uncertainty. This methodology is used, in Section V, to demonstrate the importance of quantifying the downhole detection errors and how they help, along with the real-time transmission to the surface of the seismic waveforms, to provide real-time interval velocity profiles that are consistent with postdrilling results. In Section VI, a case study that combines real-time checkshot inversion and real-time migration of downhole-to-surface transmitted seismic waveforms to optimally steer a sidetrack well so that it intersects several high-probability hydrocarbon sands is also presented before drawing conclusions in Section VII.

II. Fundamentals of Seismic Tomography

In the early phases of hydrocarbon reservoir exploration, surface seismic data are acquired with sources located near the surface of the Earth and receivers being either at the surface or at the sea floor.[1] At the exploration phase, only few wells are available (or none at all). When a potential hydrocarbon reservoir has been identified from the interpretation of the surface seismic data, more wells are drilled to confirm the existence of a reservoir and to evaluate its economical value. If economically viable reservoirs exist, many more wells (dozens to thousands, depending on the size of the reservoirs) will be drilled to develop and to produce the hydrocarbon resources. Since they are thousands of feet below the ground, seismic data are often the only way, while drilling, to assess the 3-D geological structures surrounding the wellbore being drilled. Although Earth models are physically represented in spatial coordinates, seismic data are recorded in time. It is thus critical to obtain, throughout the drilling process, accurate measurements that support the mapping of seismic times into depth values. Such a transformation is known as seismic tomography. It consists of determining the velocity model that describes the speed at which seismic waves propagate inside the targeted subsurface model.

Earth velocity models contain a wide range of wavelengths. At the seismic scale, they can be decomposed into a low-frequency (long wavelengths of about hundreds of meters) component and a high-frequency model (short wavelengths of about few meters) of velocity contrasts (as illustrated in Fig. 2). Claerbout [10] shows that the information related to the travel times of seismic waves is mostly controlled by the low frequency of the velocity models, while the high-frequency contrasts contribute to the determination of the seismic amplitudes.

Earth models are elastic and potentially anisotropic. Elastic wave equations are used to describe the propagation inside such media of compressional (also referred in seismology as primary, P-) and shear (secondary, S-) waves. Their solutions contain both phase (i.e., travel-time evolution) and amplitude information. Because compressional waves have a higher velocity than their associated shear waves, they arrive first at receiver locations. Consequently, P-wave travel times are easier

[1]The receivers are typically three-component sensors measuring, in three directions, the displacements of the seismic waves arriving at the receiver. Explosive airgun sources are typically used for marine exploration, while vibrator sources are normally used on land. The useful frequencies of those sources are up to about 250 Hz.

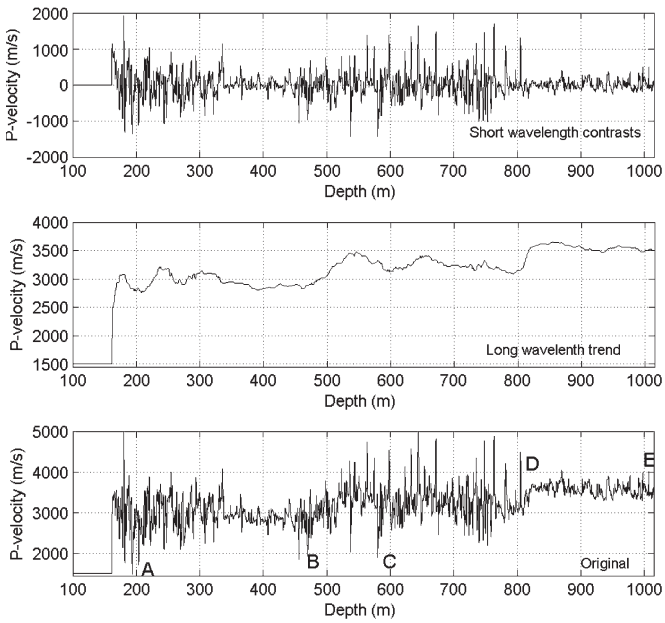

Fig. 2. Typical subsurface velocity profile (bottom) decomposed into a low-frequency trend (middle) and a high-frequency contrast model. Whereas the velocity contrasts help to determine the amplitudes of seismic waves that propagate inside the medium, the long wavelengths of the velocity model control their propagation travel times. Knowing that seismic data are always recorded in time, seismic tomography consists of inferring the subsurface depth velocity profile, allowing a correct time-to-depth mapping. It is used, in real time while drilling, to invert checkshot measurements and to monitor the geometry path of the borehole being drilled in depth using a time-recorded seismic section (or volume) as background visualization (see Fig. 1). Note the depths of the five reflectors labeled A–E.

to be detected on the seismograms than the S-wave travel times. They are thus primarily used for seismic tomography.

Following, for instance, [11] and under asymptotic approximation, it can be shown that the travel times of seismic waves satisfy the Eikonal equation so that

$$\nabla^2 t(\mathbf{x}) = \frac{1}{c(\mathbf{x})}. \tag{1}$$

Here, only compressional waves are considered, with $c(\mathbf{x})$ representing the P-wave velocity at a given location $\mathbf{x}$ of the subsurface medium.

If one considers only vertically propagating waves, then time (t) and depth (z) are linked by

$$z = \int_0^t c(t')dt' \qquad t = \int_0^z \frac{1}{c(z')}dz'. \tag{2}$$

Prior to investigating the potential sources of uncertainty that might be associated with real-time checkshot measurements, let us first illustrate the impact of inaccurate velocity models on seismic time-to-depth mapping. Given a velocity model, the one-way travel time associated with each depth can be calculated using (2). The curve labeled 0% in Fig. 3(a) shows the time-versus-depth curve corresponding to the 1-D velocity model displayed in Fig. 2. The other curves in this figure represent the time–depth curves obtained assuming errors in the original velocity model. These relative errors range from -20% to $+20\%$, with 5% increment. At the origin, the absolute depths are equal to zero since there is no wave propagation yet. The deviation between the different time–depth curves significantly increase with increasing propagation times. For instance, the exact depths of the five reflectors labeled A–E in Fig. 2 are 203.50, 456.25, 580.25, 804.87, and 997.50 m, which correspond to one-way travel times (assuming vertical propagation) of 0.1225, 0.2090, 0.2485, 0.3188, and 0.3731 s, respectively. As illustrated in Fig. 3(b), when, for instance, a $+10\%$ relative velocity error might appear *a priori* reasonable, this would lead to depth errors of 20.350, 45.625, 58.025, 80.487, and 99.750 m on the position of reflectors A–E, respectively. Clearly, more accurate velocity models result in better optimization of real-time operations and better drilling risk management.

III. SWD Data Analysis

A. Origin of Clock Drift Uncertainty

Until recently, a major source of uncertainty associated with checkshot data acquired while drilling has been the relative drift of the clock embedded with the tool downhole compared with the clock at the surface. As shown in Fig. 1, a synchronized clock system is used to acquire seismic MWDs. One clock measures the firing time of a surface source near the well head, while a second clock, which is contained within the downhole tool, collects the first arrival time of acoustic waves traveling directly from the source to the downhole receiver. The time measured is then transmitted to the surface through mud-pulse telemetry. If the two clocks were perfectly synchronized, the desired OWT would then be obtained by simply differentiating the times measured with the two clocks. Unfortunately, the clock embedded downhole with the tool drifts with respect to the uphole clock, causing an unknown systematic error on the transit time data. In such cases, the uncertainties associated with the time observations can no longer be assumed random and uncorrelated among samples. Those drifts are not predictable. They are caused by several factors, including the high temperature and pressure downhole and the shocks received by the tool while drilling (e.g., [12]). They are measured in particles per billion (ppb) and, for many years, could be as large as ± 15 ppb, depending on manufacturer specifications. (As we will see later, today's average clock drifts are about 2 ppb and rarely exceed 4 ppb.) For instance, a 15-ppb clock drift over five days of drilling would lead to 6.4-ms time error. Such errors cannot be neglected when considering the seismic wave frequencies used to build the long wavelengths of the reservoir velocity model. When the tool is brought back to surface, the actual drift is measured by resynchronizing with GPS time, and a linear correction is applied to the data. However, during drilling a large clock drift can have a significant effect on the calculated interval velocities, particularly when the rate of penetration is very low.

B. Origin of Downhole Time-Picking Errors

The second source of uncertainty is due to the downhole acquisition and processing of the seismic waveforms. The

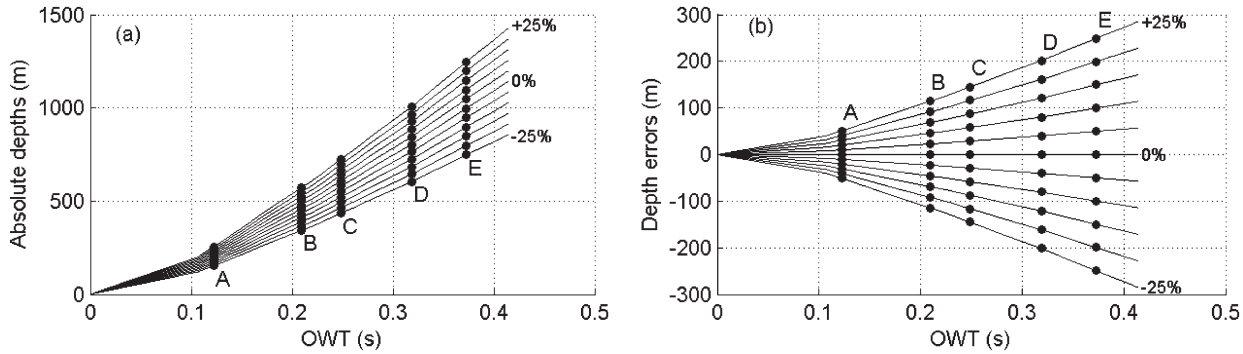

Fig. 3. Travel-time-versus-depth curves estimated by assuming a relative error in the velocity model, ranging from −25% to +25%, with 5% increment. The labels A–E shown help to illustrate how the depths of reflectors A–E, shown on the original velocity model displayed in Fig. 2, evolve with errors in the velocity model.

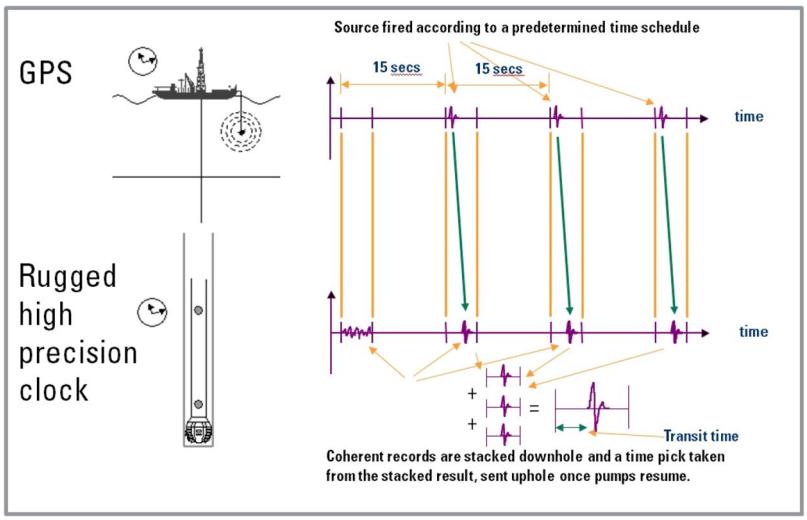

Fig. 4. Procedure for downhole acquisition timing. First, surface and downhole clocks are synchronized, and cycles begin every 15 s. Next, sources are fired at the surface according to a predetermined time schedule. The downhole sensors record seismic waveforms on a predetermined time schedule. Finally, coherent records are stacked downhole, and an OWT is picked from the stack result and sent uphole once the pumps resume.

acquisition timing is illustrated in Fig. 4. First, the tool and surface clocks are synchronized with GPS time at the surface before drilling starts. Thereafter, every 15 s, an event window occurs, and the downhole tool checks to see if the pumps are on (drilling), and if so, the tool goes back to sleep. If the pumps are off, then the tool monitors a 3-s window (which has a fixed predetermined delay from the start of the event window based on the depth of drilling and formation velocity) of the hydrophone and/or geophone data to look for incident energy. At the surface, the engineer (typically sitting in the wireline unit or in another location with a view of the rig floor) decides to fire the airguns or not. If the driller is making a connection and the downhole tool is stationary, the engineer enables the automatic-gun-firing software. This fires the airguns exactly 15 s apart at the start of each event window, controlled by GPS time. The downhole tool analyzes the incident energy, and an algorithm decides whether there is a first break or not. If a shot is deemed to be good, this is placed in a buffer. Although each shot is recorded in memory for later processing, the real-time measurement relies on at least three sequential shots to arrive at the tool at the same time offset in the window and also with the same wave shape. This is to avoid the tool triggering on noise generated by the rig. If at least three shots are seen, the tool starts to stack the waveforms and continues to stack on each firing. Once the pumps resume, the first break time is calculated from the stacked waveform and passed to the MWD telemetry to be sent uphole. Since we are downhole, the first acoustic waves that arrive at the receivers are detected using automated event detection software. These downhole measurements may suffer from errors inherent to the automatic time-picking process.

C. *Illustration With a Field Example*

To illustrate the impact that inaccurate time picking and downhole clock drift may have when estimating the formation interval velocity, let us consider *a posteriori* two checkshot data sets collected while drilling in deep water in the Gulf of Mexico (Fig. 5). For confidentiality issues, the depth origin has been reset to zero throughout this paper.

The first data set (blue curve) corresponds to the raw measurements that are collected downhole while drilling. The second (black curve) consists of the classical checkshot measurements available after drilling—or at least once the drilling tool is pulled out from the hole. The seismic waveforms are then available at the surface and can be processed by an interpreter.

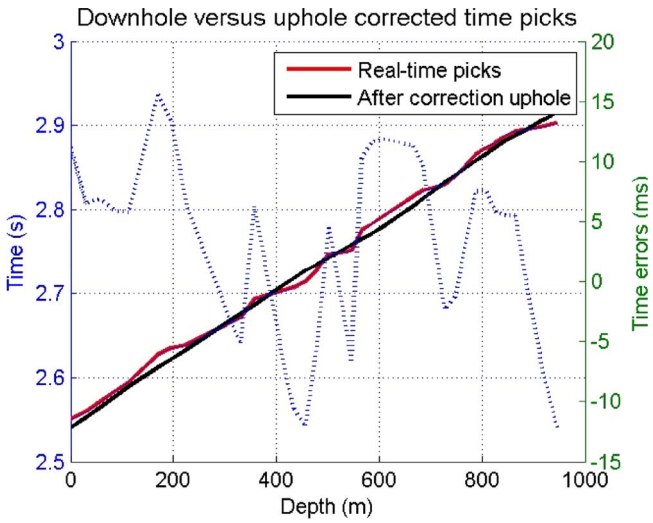

Fig. 5. Two sets of checkshot measurements are displayed. In red are the data picked in real time by automated software and transmitted to the surface through mud-pulse telemetry. In black are the transit times picked by an interpreter at the surface after the drilling tool has been pulled out and the seismic waveforms have been corrected from the clock drift. The difference between the two data sets is represented by the dotted blue line using the right axis. Note that the depth origin has been reset to zero for confidentiality purposes.

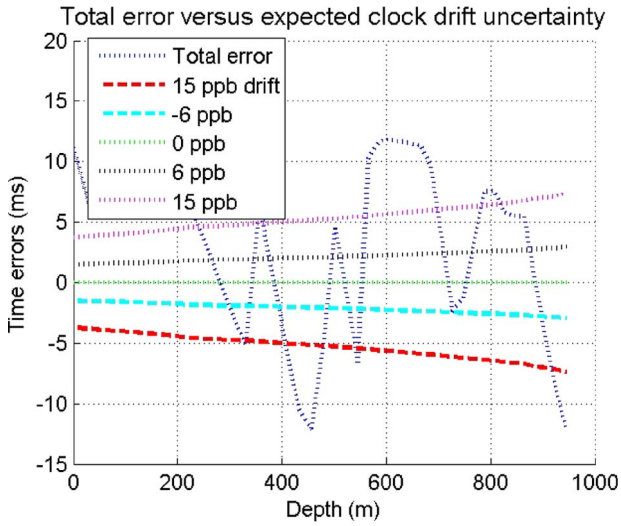

Fig. 6. Total measurement errors (dotted blue line) compared with the uncertainty that would be expected for a linear clock drift ranging from −15 to 15 ppb. Although the total error curve falls within the ±15-ppb clock drift envelope, the downhole time detection appears to be the primary source of uncertainty associated with this data set (i.e., given that the mean clock drift measured when the tool was brought back to the surface is 6 ppb.)

First, the seismograms are corrected for a linear clock drift (since the two clocks are at the surface and a mean clock drift rate can be estimated and removed from the data). Then, a borehole seismic interpreter manually picks the first arrival times for the different receiver depths. The resulting checkshot data set is thus free of linear clock drift and does not suffer from significant time-picking errors. It is thus comparable to any checkshot data set derived from a wireline VSP, except for the larger depth station spatial sampling interval (i.e., typically around 10 m for wireline as compared to around 30 m for real-time seismic MWDs).

The difference between the two data sets (blue dotted curve) are the total errors to be associated to the downhole measurements. They are plotted in milliseconds and range from −12 to 16 ms. A close insight into the measurement errors is provided in Fig. 6, where the observed data errors (blue dotted curve) are compared to a family of predicted time errors that would be observed if only a clock drift effect was present. For this specific job, an average drift of 6 ppb was measured between the two clocks when the drilling tool was brought back to the surface. This shows that, when comparing the 6-ppb drift envelope to the observed errors, in addition to the clock drift errors, there are errors induced by the automated event detection used downhole to obtain the measurements. This observation is also supported by the fact that the trend of observed errors does not increase with the acquisition time as would be expected with an exclusive clock drift effect.

Although these time errors are exceptional, i.e., not representative of the errors observed in most jobs, they are interesting from a research point of view of looking backward to illustrate in real-time checkshot measurement uncertainties and values (i.e., demonstrate in a quantitative way) how recent breakthroughs have helped reduce uncertainties in formation velocity prediction while drilling.

D. Recent Breakthroughs in Seismic Acquisition While Drilling

The precision and robustness of clocks embedded with SWD tools have significantly improved over the past years. Whereas a moderate mean clock drift of 6 ppb was observed with this job executed several years ago, today's mean drifts are about 2 ppb and rarely exceed 4 ppb. Nevertheless, clock drift uncertainty can only be resolved after the drilling is complete or when the tool is brought back to the surface.

The improvement of downhole event detection is a very active research area that is beyond the scope of this paper. References [9] and [13] proposed to make waveforms recorded in downhole memory available in real time to an interpreter uphole through mud-pulse telemetry. A major challenge is that mud-pulse telemetry has limited transmission rates of about 1–10 b/s. For instance, transmitting one float of 32 bits would require 3–32 s. Therefore, only part of the available waveforms are often sent uphole in real time. Demonstrating the value of the following is thus of great importance for successful drilling risk management: 1) transmitting in real time to the surface the recorded seismic waveforms and 2) collecting downhole checkshot measurements with their standard deviations.

IV. Method to Account for Real-Time Uncertainties While Drilling

In this section, a method is presented for inverting real-time checkshot data that contains both picking errors and clock drift uncertainty.

A. VSP Checkshot Inversion Background

Consider a typical checkshot acquisition geometry as shown in Fig. 1. Assuming a vertical incidence wave propagation and a 1-D layered Earth model regularly sampled with a depth sampling interval dz, the one-way first arrival time t^i of a

compressional seismic wave propagating from the source to the ith downhole receiver is related to the formation interval slownesses (i.e., inverse of velocities) of the K_i layers above the receiver by

$$t^i - t_o = dz \sum_{k=1}^{K_i} s_k + (z_{r_i} - K_i dz) s_{[K_i+1]} \tag{3}$$

where z_{r_i} is the depth of the ith receiver, t_o is the calibration time, and s_k is the interval slowness of the considered kth layer. Note that, since we are only interested in interval velocities, the measured OWTs are calibrated to the OWT corresponding to the top of the targeted depth interval, i.e., $d^i = t^i - t_o$. The purpose of such variable change (using d^i instead of t^i with $t_o = t^1$) is to eliminate any uncertainty related to the overburdened part of the formation where only an average velocity can be inferred from the observations.

The estimation of the formation interval slowness profile from a set of checkshot measurements can thus be expressed as a linear problem of the form

$$\mathbf{d} = \mathbf{G}\mathbf{m} \tag{4}$$

where the observation vector $\mathbf{d}$ represents the calibrated measurements for the different drilling tool stations. The vector $\mathbf{m}$ represents the model parameters and consists of the P-wave interval slownesses such that $\mathbf{m} = (s_1, s_2, \ldots, s_L)$. The matrix $\mathbf{G}$ defines the theoretical relation that maps the model to the data space.

Following [14], the solution obtained by estimating the slowness vector $\mathbf{m}$ from the observed OWTs $\mathbf{d_{obs}}$ is a Gaussian posterior probability density with center $\mathbf{m_{est}}$ and covariance operator $\mathbf{C_{M'}}$ such that

$$\mathbf{m_{est}} = \left[\mathbf{G^T C_D^{-1} G} + \mathbf{C_M^{-1}}\right]^{-1} \mathbf{G^T C_D^{-1} d_{obs}} \tag{5}$$

$$\mathbf{C_{M'}} = \left[\mathbf{G^T C_D^{-1} G} + \mathbf{C_M^{-1}}\right]^{-1}. \tag{6}$$

Here, it is assumed that uncertainties on the data and on the model parameters have Gaussian distributions. In (5) and (6), $\mathbf{C_D}$ and $\mathbf{C_M}$ are the covariance operators describing the *a priori* uncertainties on the data and on the model parameters, respectively. Typically, the *a priori* model covariance matrix ($\mathbf{C_M}$) helps control the smoothness of the inverted model (e.g., [14]–[16]).

B. Typical Sources of Real-Time Checkshot Uncertainty

In the case of real-time checkshot measurements, while the tool is still downhole during drilling, two major sources of uncertainty need to be considered.

1) Time-picking errors ($\mathbf{n_{D_{picking}}}$) are assumed to have a Gaussian distribution, to be independent among samples, and to be modeled with a diagonal covariance matrix $\mathbf{C_{D_{picking}}}$.
2) Downhole clock drift is assumed to have two components: $\mathbf{n_{D_{drift}^{linear}}}$ and $\mathbf{n_{D_{drift}^{deviations}}}$. The primary component linearly varies with the acquisition time and is considered as coherent noise that is not subtracted from the raw measurements but rather modeled as uncertainty. The second consists of the deviations around the mean drift rate after the linear clock drift is removed.

It should be noted that when the tool is still downhole, the clock drift is not predictable, and a total resolution of the clock drift uncertainty will occur only after the drilling is complete.

The data noise is thus the sum of three random noise sources

$$\mathbf{n_D} = \mathbf{n_{D_{picking}}} + \mathbf{n_{D_{drift}^{linear}}} + \mathbf{n_{D_{drift}^{deviations}}}. \tag{7}$$

The data covariance matrix $\mathbf{C_D}$ is therefore obtained by summing the covariance matrices associated with the different uncertainties

$$\mathbf{C_D} = \mathbf{C_{D_{picking}}} + \mathbf{C_{D_{drift}^{linear}}} + \mathbf{C_{D_{drift}^{deviations}}}. \tag{8}$$

C. Accounting for Deviations Around the Linear Clock Drift Model

In this section, the covariance matrix required for properly accounting for the clock drift uncertainty is derived. In particular, it will be very useful for inverting the transit times picked from seismic waveforms recorded downhole and transmitted to the surface while the tool is still downhole. That is, the transit times can accurately be picked by an interpreter but will still suffer from the clock drift uncertainty.

Let us assume that the clock drift is linear with time and can be represented by a drift rate denoted as β. The measured OWTs can then be expressed as

$$t^i = t^i_{\mathrm{OWT}} + \beta \left(t^i_{\mathrm{shot}} - t_{\mathrm{cali}}\right) \tag{9}$$

where t^i_{shot} is the time where the source has been emitted, t^i_{OWT} is the OWT that would be recorded if no uncertain clock drift was present, and t_{cali} is the last time when the two clocks were synchronized.

In this case, the covariance matrix $\mathbf{C_D}$ describing the uncertainty associated with the time observations will no longer be diagonal since it will represent both the errors associated with the random (uncorrelated among samples) noise and the ones related to the coherent time-dependent clock drift. By definition, the covariance between the ith and jth data samples can be expressed as

$$\mathrm{Cov}(t^i, t^j) = E\left(\left(t^i - \langle t^i \rangle\right)\left(t^j - \langle t^j \rangle\right)\right). \tag{10}$$

Inserting the expression of t^i as defined in (9) into (10) leads after some algebra to

$$\begin{aligned}\mathrm{Cov}(t^i, t^j) = &\mathrm{Cov}\left(t^i_{\mathrm{OWT}}, t^j_{\mathrm{OWT}}\right) \\ &+ \left(t^i_{\mathrm{shot}} - t_{\mathrm{cali}}\right) \mathrm{Cov}\left(t^i_{\mathrm{OWT}}, \beta\right) \\ &+ \left(t^j_{\mathrm{shot}} - t_{\mathrm{cali}}\right) \mathrm{Cov}\left(t^j_{\mathrm{OWT}}, \beta\right) \\ &+ \left(t^i_{\mathrm{shot}} - t_{\mathrm{cali}}\right)\left(t^j_{\mathrm{shot}} - t_{\mathrm{cali}}\right) \mathrm{Cov}(\beta, \beta).\end{aligned} \tag{11}$$

Since there is no correlation between t^i_{OWT} and β, we have $\mathrm{Cov}(t^j_{\mathrm{OWT}}, \beta) = 0, \forall i$. Thus, the covariance between the ith and jth data samples in the presence of clock drift is

$$\begin{aligned}\mathrm{Cov}(t^i, t^j) = &\mathrm{Cov}\left(t^i_{\mathrm{OWT}}, t^j_{\mathrm{OWT}}\right) \\ &+ \left(t^i_{\mathrm{shot}} - t_{\mathrm{cali}}\right)\left(t^j_{\mathrm{shot}} - t_{\mathrm{cali}}\right) \mathrm{Var}(\beta).\end{aligned} \tag{12}$$

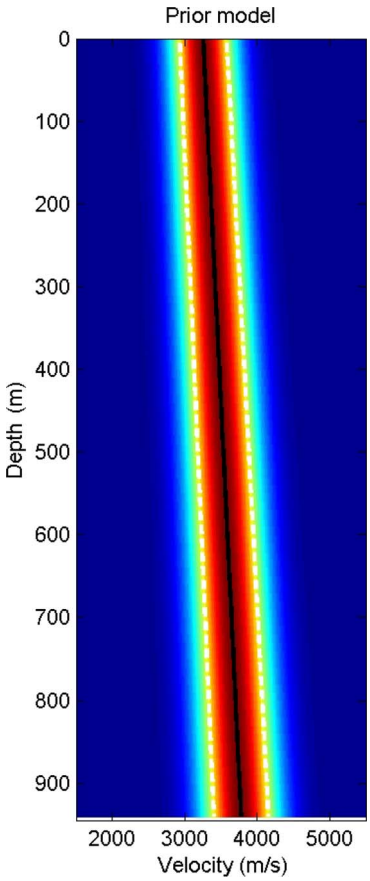

Fig. 7. Same prior model, assuming a linear variation of the velocity with depth, is used for all of the following inversions.

When considering the calibrated data (it is assumed here that calibration is made according to the first receiver depth, i.e., $t_o = t^1$), the data sample d^i can then be expressed as

$$\begin{aligned} d^i &= t^i - t_o \\ &= \left[t^i_{\mathrm{OWT}} - t^1_{\mathrm{OWT}}\right] + \beta\left(t^i_{\mathrm{shot}} - t^1_{\mathrm{shot}}\right). \end{aligned} \tag{13}$$

The data covariance matrix $\mathbf{C_D}$ is thus a nondiagonal matrix whose element $C_D(i,j)$ can be expressed similarly to (13) by the following:

$$\begin{aligned} C_D(d^i, d^j) = &\operatorname{Cov}\left(d^i_{\mathrm{OWT}}, d^j_{\mathrm{OWT}}\right) \\ &+ \left(t^i_{\mathrm{shot}} - t^1_{\mathrm{shot}}\right)\left(t^j_{\mathrm{shot}} - t^1_{\mathrm{shot}}\right)\operatorname{Var}(\beta). \end{aligned} \tag{14}$$

V. Gulf of Mexico Checkshot Inversion Results

Three scenarios have been considered with the following assumptions.

1) The downhole time-picking errors cannot be estimated or sent in real time to the surface.
2) The downhole time-picking errors can be estimated downhole and sent to the surface along with the picked times for integration in the inversion scheme.
3) The seismic waveforms can be made available at the surface despite the cost in mud-pulse telemetry.

The results of the experiments performed with data from deep water in the Gulf of Mexico, using the same prior velocity model shown in Fig. 7, are displayed in Fig. 8. The linear clock

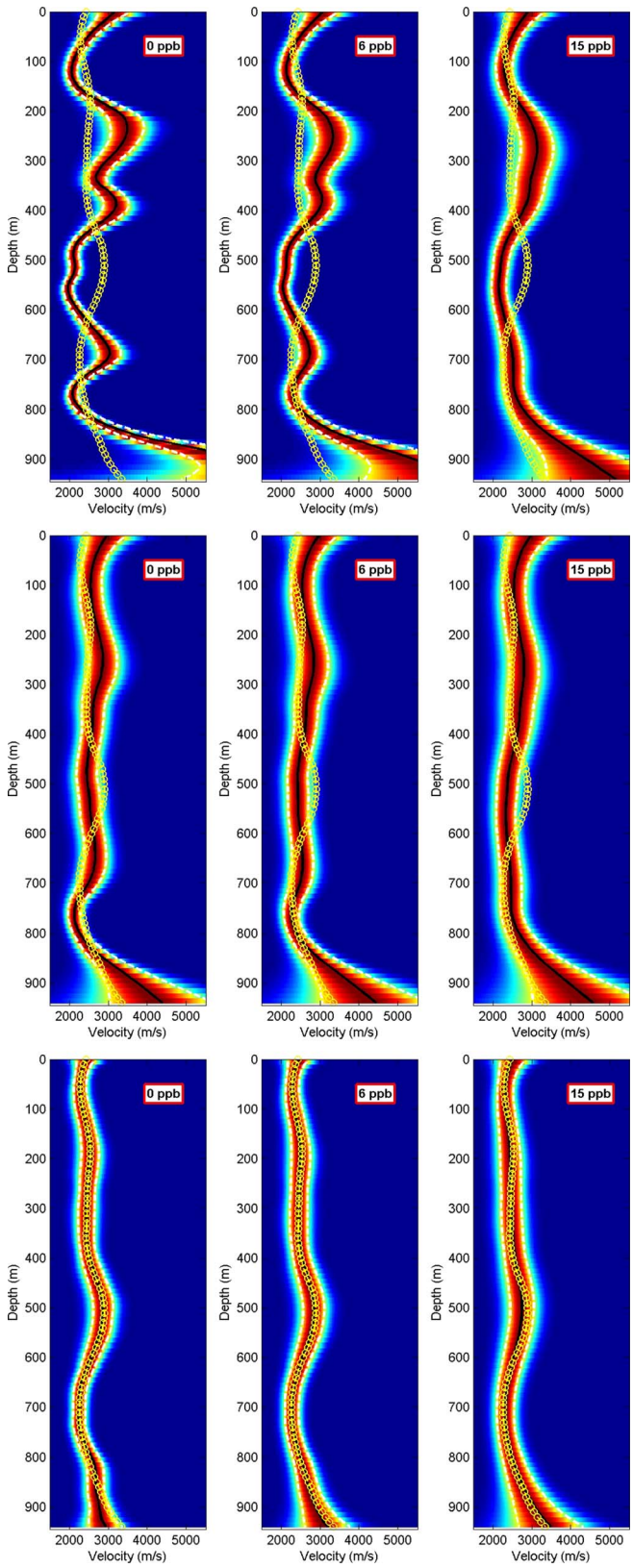

Fig. 8. Top: Inverted velocity models assuming downhole time-picking errors not available in real time. Middle: Downhole time-picking errors are quantified in real time and incorporated in the time-picking covariance matrix. Bottom: Seismograms recorded downhole are sent uphole in real time for an accurate time picking by a borehole seismic specialist. For each mean clock drift considered, the true profile is compared to the estimated most likely models overlaid in black. Note that the mean clock drifts today are about 2 ppb and rarely exceed 4 ppb.

drift is assumed unknown since drilling is progressing in real time. We browse the range of possible clock drifts with the two extreme values, i.e., 0 and 15 ppb, in addition to 6 ppb, which is a moderate drift rate that appears to be the value observed after drilling in the case of the deep water in the Gulf of Mexico. The standard deviation around a given clock drift rate is chosen as 3 ppb. The most likely velocity profile obtained after drilling is complete (i.e., after being corrected for the clock drift and having the OWT accurately picked by an interpreter) is overlaid as the dashed-yellow-circle curve on all the inverted models as the correct profile.

In the top row of Fig. 8, the real-time downhole picks are inverted assuming that the downhole time-picking errors can neither be quantified nor sent in real time to the surface. These errors are defaulted to a Gaussian distribution of zero mean and 2-ms standard deviation. For most depths, the expected correct profile is clearly largely outside the estimated *a posteriori* uncertainty bounded velocity range. In other words, this shows that, defaulting the downhole picking standard deviation error to 2 ms, the nominal time resolution of the recorded seismic waveforms may lead to meaningless posterior uncertainties on the real-time interval velocity profiles.

In the middle figure, the same downhole real-time picks are inverted. However, now, their associated errors have been integrated in the inversion framework via the time-picking covariance matrix. Clearly, this helps to output better mean interval velocity profiles with more meaningful *a posteriori* uncertainties, in which the correct model now fits quite well, except for a few drilling tool positions such as around 520-m depth.

The downhole picking accuracy can be quite poor, depending on the data quality and the downhole filtering applied. For example, applying a zero-phase downhole filter creates precursory arrivals before the first break, whereas a minimum-phase filter tends to delay the main energy, making the first break hard to identify in the presence of noise. This is one reason why there is a need for real-time waveform data. However, at the time when these data were acquired, the system for transmitting the full seismic waveforms through mud-pulse telemetry while drilling was not implemented. Thus, we simulate synthetic data by adding to the uphole corrected measurements (Fig. 5, black curve) clock drift time errors modeled with a Gaussian distribution with 6-ppb mean and 3-ppb standard deviation. With the bottom figure, the value of transmitting the seismograms in real time to the surface for an accurate time picking by an interpreter is demonstrated. Indeed, the *a posteriori* uncertainties associated with the real-time inverted velocity model are significantly reduced. In addition, the most likely inverted profile matches the expected correct one very well as long as the clock drift is properly accounted for. This is shown, for instance, with the bottom-right figure with 15-ppb clock drift envelope.

In the next section, we show a field example where the real-time inverted velocity profile is used to migrate seismic waveforms transmitted to the surface while drilling and how this helps for evolving the drilling strategy, as required, in a timely and cost-effective manner.

VI. Gulf of Mexico Look-Ahead Example

In this field example, SWD VSP data were being acquired on the Gulf of Mexico shelf to optimally position the wellbore near a fault, which was imaged from existing surface seismic data. More specifically, we wish to use real-time information to accurately steer the well so that it intersects several targeted hydrocarbon sands that are trapped by the fault barrier (Fig. 9). One way to achieve such objectives is to drill the well, according, for instance, to a predrill plan, and to stop drilling every time that wireline checkshot surveys need to be performed to collect additional seismic measurements. Stopping the drilling implies loss of rig time, which might cost about $200 000 per day.

The main difficulties assessed were the following:

1) high risk of lost rig time;
2) high risk of abrupt velocity changes in this area;
3) high risk of no well control up-dip close to the fault;
4) high risk of no time-versus-depth control below the fault.

These risks were mitigated by alternatively adopting an SWD technology[2] with the following objectives:

1) to real-time steer one well, with a possible sidetrack well, to optimally reach the potential reservoir targets;
2) to timely assess the sidetrack well option and decide when it is deemed to implement it;
3) to adequately set casing strings to maximize future production;
4) to avoid excessive lost rig time and associated costs.

That is, real-time checkshot data were acquired while drilling to accurately estimate the interval velocity profile for a reliable time–depth mapping. In addition, real-time seismic waveforms were transmitted uphole so that they can be processed and migrated, thus providing look-ahead depth images from which better drilling decisions can be made. Fig. 10 shows some of the waveforms transmitted, via mud telemetry, to the surface while drilling the well above 11 780-ft depth. While the first target was predicted at 10 876-ft true vertical depth (TVD) according to the predrill plan, real-time information provided by the checkshot data inversions allows for continuous time–depth mapping updates. For instance, the first target was penetrated at 11 177-ft TVD (+301 ft away from the predrill prediction) after being appropriately updated to 11 034, 11 059, and 11 107 ft, when drilling reached 10 500, 11 000, and 11 500 ft, respectively.

The real-time waveforms and the images obtained after their depth migration are displayed in Fig. 11. Although the drilling has not yet reached the deepest targeted horizons, one can already see them ahead of the drill bit. Due to the large velocity changes observed from the checkshot-based interval velocity profiles, it was adopted to drill a sidetrack well to reach the deepest horizons (instead of continuing on the first well track). Fig. 12 provides the final depth image obtained after migrating

[2]The sources are airguns, which are fired 62 ft from the well head. For each source firing, 18 levels (one of two) of downhole receivers are recorded and transmitted to the surface via high-speed telemetry. The total set of 39 traces is recorded in the tool memory and is available every time the tool is brought to the surface. The total acquisition and transmission time (per source firing) is about 1 h. The real-time checkshot measurements (one single time value per downhole receiver) is transmitted to the surface in about 5 min. At 3 b/s, a 600-ms waveform typically takes 40 min to be received at the surface. It takes a further 20 min for the well-site processing software to update the VSP processing. All data transmitted to the surface were also transmitted by satellite to geophysical experts remotely located in town.

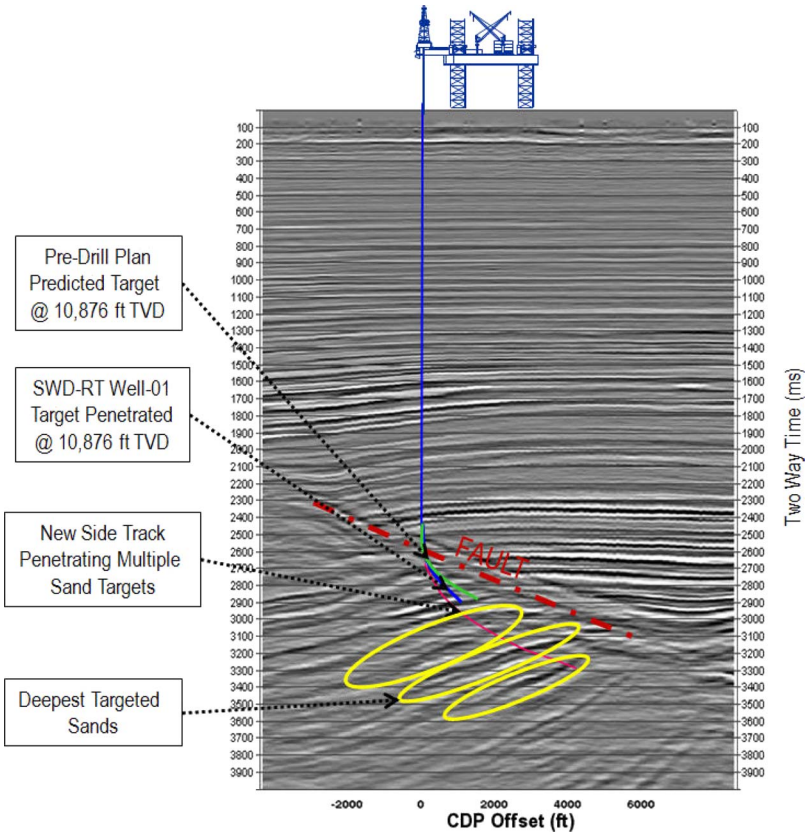

Fig. 9. Examples of real-time waveforms, collected for different depth positions and at different dates, showing a clear consistency of the source wavelet shape as a function of acquisition time.

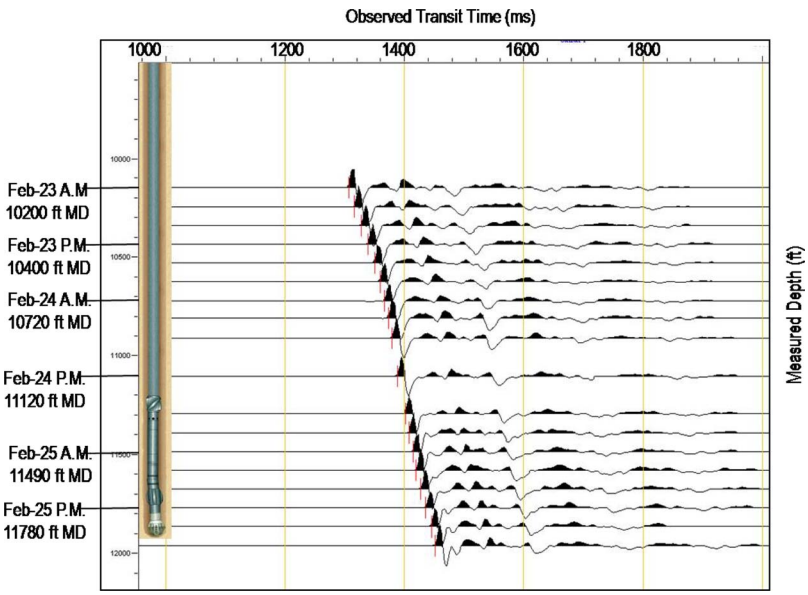

Fig. 10. Examples of real-time waveforms, collected for different measured depth (MD) positions and at different dates, showing a clear consistency of the source wavelet shape over acquisition times.

the seismic waveforms acquired in both the first and sidetrack wells. An overlay on the surface seismic section (Fig. 13) clearly shows consistent ties (in terms, for instance, of horizon alignment) with the surface seismic.

As summarized in Fig. 9, where the predrill plan, the two actual drilled well tracks, the fault barrier, and the targeted high-probability hydrocarbon reservoirs are displayed, this successful SWD project helps in obtaining the following real-time achievements.

- Wireline-conveyed checkshots are avoided.
- Multiple pay sands intersected as required.
- No rig time is used due to real-time seismic operations.
- The wellbore trajectory changed as needed; the well was seismically steered.

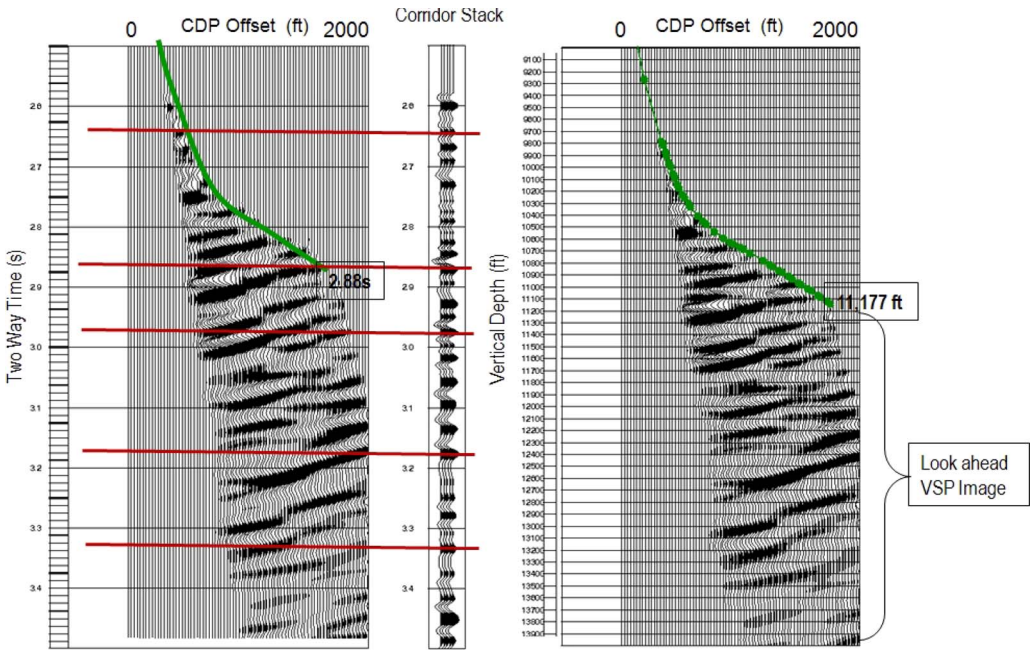

Fig. 11. Time and depth look-ahead images after drilling the first well. A decision was then made, based on the real-time inverted velocity profiles and the look-ahead information, to drill a sidetrack well to better intersect the targeted hydrocarbon sands.

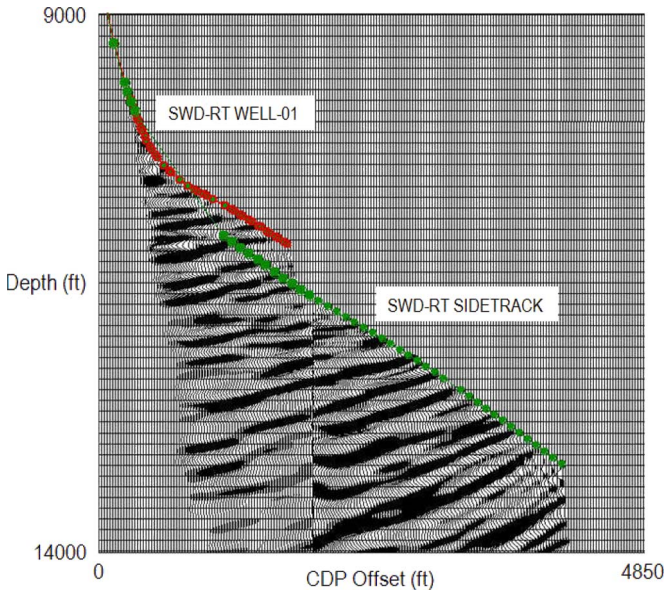

Fig. 12. Depth image obtained after migrating, using the real-time inverted velocity profile, the seismic waveforms collected from the two wells in consideration.

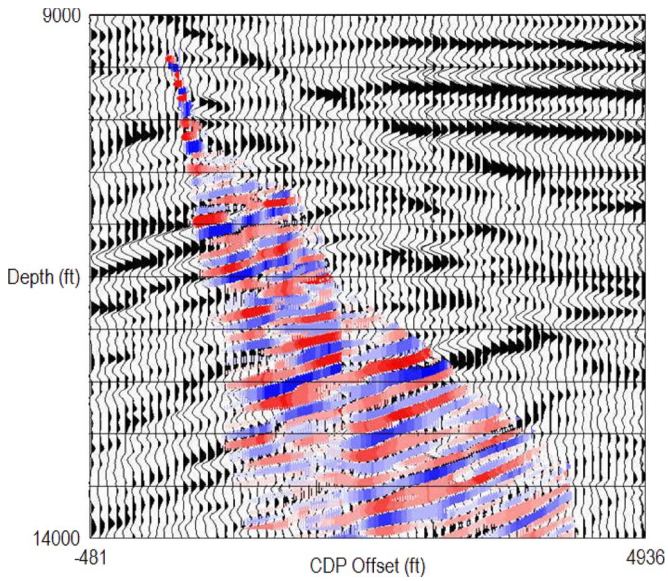

Fig. 13. Real-time-obtained vertical-incidence VSP image overlaid on the predrilling surface seismic section.

- Real-time (and recorded-mode) migrated images confirmed seismic amplitudes associated with the targeted hydrocarbon sands.
- The early sidetrack decision saved seven days of rig time and more than $1 400 000.

VII. Conclusion

The seismic measurements and formation interval velocity surrounding the wellbore are key elements that are desirable to access in real time with uncertainty while drilling. It has been shown, by analyzing a data set acquired in deep water in the Gulf of Mexico, that real-time checkshot may suffer from large downhole time detection errors in addition to an unpredictable clock drift uncertainty. We have developed a method to account for these uncertainties and to provide drillers with reliable formation interval velocity models in real time. In addition to the typical parameters needed for wireline checkshot inversion, two more variables, i.e., the expected linear clock drift rate and its variance, are required for real-time checkshot data inversion with uncertainty. We have then demonstrated that quantifying in real time the downhole time detection errors, rather than defaulting them to 2 ms (which is the nominal time sample interval of the recorded waveform), helps to provide consistent real-time velocity models that are comparable to the profile

obtained from travel times picked after drilling by a human interpreter.

The ability to record and transmit waveforms to the surface during borehole seismic acquisition is a major step forward in seismic LWD technology. We have shown that inverting the checkshot data picked from the real-time transmitted seismic waveforms can significantly reduce the uncertainties associated with the real-time inverted velocity profiles, even if there might be an associated telemetry cost. Moreover, real-time transmission allows for both visual quality control of the data and the possibility to process and migrate them for looking ahead in real time as drilling continues. This negates the need to wait for the tool to be brought to the surface before accessing these waveforms for effective drilling risk management.

ACKNOWLEDGMENT

The authors would like to thank Associate Editors Prof. D. Petri and Prof. A. Ferrero and the two anonymous reviewers for their useful comments. They would also like to thank Schlumberger for the permission to publish this paper.

REFERENCES

[1] H. Djikpesse, "Valuing recent advances in seismic-while-drilling applications by estimating uncertainty reduction in real-time interpreted velocity measurements," in *Proc. IEEE Int. Workshop Adv. Methods Uncertainty Estimation Meas.*, Jul. 21–22, 2008, pp. 96–101. Digital Object Identifier 10.1109/AMUEM.2008.4589942.

[2] R. A. Stephen and A. J. Harding, "Travel time analysis of borehole seismic data," *J. Geophys. Res.*, vol. 88, no. B10, pp. 8289–8298, 1983.

[3] J. Pujol, R. Burridge, and S. B. Smithson, "Velocity determination from offset vertical seismic profiling data," *J. Geophys. Res.*, vol. 90, no. B2, pp. 1871–1880, 1985.

[4] R. R. Stewart, "VSP interval velocities from traveltime inversion," *Geophys. Prospect.*, vol. 32, no. 4, pp. 608–628, 1984.

[5] G. T. Schuster, D. P. Johnson, and D. J. Trentman, "Numerical verification and extension of an analytical generalized inverse for common-depth-point and vertical-seismic-profile traveltime equations," *Geophysics*, vol. 32, pp. 608–628, 1988.

[6] D. Lizarralde and S. Swift, "Smooth inversion of VSP traveltime data," *Geophysics*, vol. 64, no. 3, pp. 659–661, May/Jun. 1999.

[7] A. Malinverno and V. A. Briggs, "Expanded uncertainty quantification in inverse problems: Hierarchical Bayes and empirical Bayes," *Geophysics*, vol. 69, no. 4, pp. 1005–1016, Jul./Aug. 2004.

[8] C. Durrand, T. Skeryanc, C. Deri, and A. Hawthorn, "Drilling in time: Geosteering a well using real-time borehole seismic measurements: A case history from the Gulf of Mexico," in *Proc. Soc. Exploration Geophysicists Annu. Meeting, Expanded Abstract*, 2005, pp. 487–489.

[9] A. Hawthorn, C. Esmersoy, and A. L. Collins, "System and method for determining downhole clock drift," U.S. Patent 6 912 465, Jun. 28, 2005.

[10] J. F. Claerbout, *Imaging the Earth's Interior*. Cambridge, MA: Blackwell Scientific Publications, Inc., 1985.

[11] C. Chapman, *Fundamentals of Seismic Wave Propagation*. Cambridge, U.K.: Cambridge Univ. Press, 2004.

[12] G. Althoff, B. Corninsh, G. Varsamis, B. Kavaipatti, A. Arian, L. T. Wisniewski, J. O. Blanch, and A. C. Cheng, "New concepts for seismic surveys while drilling," presented at the Society Petroleum Engineers, Annu. Meeting, Houston, TX, 2004, Paper SPE 90751.

[13] C. Esmersoy, A. Hawthorn, C. Durand, and P. Armstrong, "Seismic MWD," *Lead. Edge*, vol. 24, no. 1, pp. 56–62, 2005.

[14] A. Tarantola, "Inverse problem theory," in *Methods for Data Fitting and Model Parameter Estimation*. Amsterdam, The Netherlands: Elsevier, 1987.

[15] H. A. Djikpesse and A. Tarantola, "Multiparameter l_1 norm waveform fitting: Interpretation of Gulf of Mexico seismograms," *Geophysics*, vol. 64, no. 4, pp. 1023–1035, Jul./Aug. 1999.

[16] H. A. Djikpesse, W. Meghirbi, I. Nizkous, and D. Cao, "Borehole-guided AVO analysis of P-P and P-S reflections: Quantifying uncertainty on density estimates," *Geophys. Prospect.*, vol. 54, no. 5, pp. 515–523, 2006.

Hugues Djikpesse (M'08) received the B.S. degree in applied physics from the University of Paris, Paris, France, in 1990 and the M.S. and Ph.D. degrees in earth sciences from the Institut de Physique du Globe de Paris, Paris, in 1992 and 1996, respectively.

From 1995 to 1997, he was with Total Research, Saint-Remy les Chevreuses, France, working on a field-driven 3-D anisotropic wave propagation modeling project. From 1997 to 2001, he was with Jason-Geosystems, The Netherlands, where he led their R&D effort for quantitative 3-D seismic reservoir characterization. In 2001, he joined Schlumberger K.K., Tokyo, Japan. Since 2004, he has been with the Department of Mathematics and Modeling, Schlumberger-Doll Research Center, Cambridge, MA, where he is currently a Principal Research Scientist. His current work focuses on subsurface imaging from multilevel seismics, production optimization, and risk management. He is the holder of several patents. He is the author of several commercial softwares and a dozen of peer-reviewed publications.

Phil Armstrong received the Master's degree in physics from Oxford University, Oxford, U.K., in 1981.

He is currently with the Department of Acoustics Instrumentation, Schlumberger, Tokyo, Japan. His career with Schlumberger has mostly been spent working on the analysis and processing of borehole seismic data and the development of multicomponent processing methods. He was also the Geophysicist on the team that developed the seismicVISION(tm) logging-while-drilling system. He is the holder of one U.S. patent. He is an Associate Editor and Reviewer for *Geophysical Prospecting*. His specific areas of focus included drill-bit seismic methods, borehole seismic array tools, and new applications for VSP techniques.

Dr. Armstrong is a member of the Society of Exploration Geophysicists, the European Association of Exploration Geophysicists, and the Society of Petroleum Engineers.

Rogelio Rufino received the B.S. degree in geophysics from the Instituto Politécnico Nacional, Mexico, Mexico, and the M.Sc. degree from the Centro de Investigación Científica y de Educación Superior de Ensenada, Ensenada, Mexico.

In 2000, he joined Schlumberger, Mexico, as a Junior Geophysicist. Since then, he has been working on borehole geophysics in Mexico and the U.S., processing data acquired worldwide. He is currently a Senior Geophysicist with Schlumberger Data and Consulting Services, Houston, TX. He is responsible for borehole seismic, including SWD, job planning, processing, and interpretation.

Andy Hawthorn received the B.S.(Hons.) degree in geology and the M.Sc. degree in engineering geology from the University of Durham, Durham, U.K.

In 1990, he joined Schlumberger, Norway, as a Field Engineer. Since then, he has held numerous positions around the world. He is currently the Domain Head for Acoustics and Geophysics with Schlumberger Drilling and Measurements Headquarters, Sugar Land, TX. He is responsible for the LWD sonic and seismic services, including both existing commercial and upcoming engineering and research projects.